# An Adaptive BLAST Successive Interference Cancellation Method for High Data Rate Perfect Space-Time Coded MIMO Systems

Mitchell J. Grabner , Member, IEEE, Xinrong Li , Senior Member, IEEE, and Shengli Fu, Senior Member, IEEE

Abstract-Linear dispersion (LD) based perfect space-time codes (STBCs) are an efficient means of increasing a multiple-input multiple-output (MIMO) system's overall diversity gain while maintaining the same spectral efficiency as a traditional spatial multiplexed (SM) MIMO system. Because the decoding procedure of LD codes traditionally requires the entire code to be received and decoded simultaneously, complexity increases proportional to the square of the MIMO array size. In this paper, we leverage the increased number of spatial and temporal layers at the decoder to dynamically reduce the complexity of a BLAST optimum ordering and successive interference cancellation (SIC) detector based on the instantaneous system capacity and data rate. The novel approach proposed in this paper is channel code and modulation agnostic, meaning the underlying constellation can be HEX or QAM and there is no feedback from a forward error correction (FEC) decoder, which makes the design useful in a wide range of MIMO systems employing LD codes with linear detectors. We investigate the method's bit error rate (BER) using MIMO dimensions up to  $8 \times 8$  and bits per channel use (BPCU) up to 32. We analyze the system's run-time complexity and BER performance in software and implement perfect coding along with the novel method presented here in a custom MIMO orthogonal frequency division multiplexing (OFDM) system and test it over-the-air using an Ettus Research X310 software-defined radio (SDR) testbed.

Index Terms—MIMO, OFDM, space-time codes, Interference cancellation, SDR.

# I. INTRODUCTION

THE space-time block codes (STBC) following the perfect-coding principle are a new class of linear dispersion (LD) codes that are designed to achieve the optimum multiplexing-diversity trade-off introduced by Zheng and Tse in [1]. The  $2\times 2$  case was found in [2] and [3] concurently using cyclic division algebras, the  $4\times 4$  case was found in [4] (along with 3 and 6 antennas) and  $8\times 8$  was found in [5] (along with rectangular designs) by using a non-norm unit-magnitude element. For an STBC to be considered perfect it must: 1) be full rate, hence for

Manuscript received June 10, 2019; revised September 16, 2019 and October 24, 2019; accepted October 27, 2019. Date of publication November 18, 2019; date of current version February 12, 2020. The review of this article was coordinated by Prof. W. Choi. (Corresponding author: Mitchell Grabner.)

M. J. Grabner is with the Department of Electrical Engineering, University of North Texas, Denton, TX, 76207 USA, and also with the ORAU Journeyman Fellow with the US Army Research Laboratory (ARL), Aberdeen Proving Ground, MD, 21005 USA (e-mail: mitchellgrabner@my.unt.edu).

X. Li and S. Fu are with the Department of Electrical Engineering, University of North Texas, Denton, TX, 76207 USA (e-mail: xinrong.li@unt.edu; shengli.fu@unt.edu).

Digital Object Identifier 10.1109/TVT.2019.2954207

some  $n \times n$  LD code it must transmit  $n^2$  information symbols, 2) have a nonzero minimum determinant, which gives a nonzero lower bound on the coding gain making it fully diverse, 3) constellation is shaped such that no extra energy is used for any linear combination of information symbols compared to uncoded, and 4) all coded symbols have the same average energy [6].

The incredible diversity gain performance of perfect codes is dependent on the receiver employing some sort of maximum likelihood (ML) detection criteria [6] like lattice searching [7] or sphere decoding [8]. In our previous work [9], we analyzed perfect codes up to  $8 \times 8$  with and without forward error correcting codes (FEC) and found that they maintain much of their diversity gain at fixed data rates while only using sub-optimum MMSE linear detection with and without BLAST style optimum ordering and successive interference cancellation (SIC). This corroborates the findings of [1] that an MMSE filter-based coded BLAST (in their case D-BLAST) theoretically approaches the optimum trade-off. Because the LD coding structure of perfect codes spreads the information symbols across all n spatial dimensions and n time dimensions, coherent decoding requires the information from all of the receive antennas and n channel uses. This increases the complexity significantly versus traditional spatial multiplexing (SM) systems as the received signal space-time vectors are now size  $n^2$  versus n. Much research has been conducted recently on both the transmitter and receiver in reducing the ML decode complexity of STBCs [10] as well as designing new codes which are fast decodable but with a relaxed rate [11]–[14] and/or have reduced peak-to-average power ratio (PAPR) [15], [16] which saves power in the transmit power amplifier (PA). This research takes a slightly different approach and assumes that in a real system, operating above the theoretical capacity of the fading channel is typical and there is a target error rate that needs to be met. The increased received signal dimensionality of LD codes can then be utilized to tune the receiver to meet this target while simultaneously providing much of the STBC diversity gain performance with reduced complexity. Additionally, the method presented in this research is STBC, FEC and modulation agnostic, being fully self-contained in the detector. Therefore, if a high dimension system also requires low power operation, for example, Integer Codes (ICs) can be used instead of perfect codes, with the only modification being the IC specific generator matrix stored in the receiver's device memory. This modularity means that integrating our adaptive method into future full dimension MIMO systems such as LTE

0018-9545 © 2019 IEEE. Personal use is permitted, but republication/redistribution requires IEEE permission. See https://www.ieee.org/publications/rights/index.html for more information.

A-PRO [17], 5 G uplink random access [18] or wireless local area networks (WLAN) requires minimal system or baseband digital signal processing (DSP) modification. However, massive MIMO 5 G downlink beamforming efforts which utilize an ultra-high antenna count at the base station and envision mostly *dumb* clients with a single antenna would see little benefit.

For our contributions in this paper, we leverage the increased number of space-time layers at the receiver to develop a novel adaptive perfect-coded MMSE BLAST-based optimum ordering and SIC receiver design that can dynamically change the diversity advantage of the receiver without feedback from a FEC decoder, which also reduces its complexity at very high SNR. We analyze the bit error rate (BER) over various tuning values and compare them to traditional SM systems with the same spectral efficiency and linear receiver based on extensive simulation results. We also analyze the system's run-time complexity in software by implementing it in C++11 and comparing it with various SM systems using the same bits per channel use (BPCU). To demonstrate its usefulness in practice, we further implement the novel adaptive MMSE BLAST method using a custom MIMO orthogonal frequency division multiplexing (OFDM) system that we have developed with the GNU Radio SDR framework [19] and the Ettus Research USRP hardware platform [20] and analyze the experimental over-the-air BER results compared to a baseline SM system. To the best of our knowledge, this is the first publicly demonstrated over-the-air MIMO OFDM and perfect-coded system implemented in the GNU Radio SDR framework.

The remainder of the paper is organized as follows: Section II briefly presents the MIMO system model and perfect code construction for up to 8 dimensions. Section III reviews the linear MMSE BLAST decoding process (optimum ordering and SIC) for LD-based STBCs. Section IV details our novel adaptive SIC method using the data rate of the system and the instantaneous capacity of the channel. Section V explains the simulation and software development environments and presents the complexity and BER results obtained for the systems with different antenna array sizes. Section VI explains the implementation of perfect coding and the novel detector using custom MIMO OFDM in the GNU Radio SDR framework and presents the experimental over-the-air performance results on a coherent MIMO testbed using the Ettus Research X310. Finally, we conclude in Section VII.

### II. SYSTEM MODEL AND CODE CONSTRUCTION

The system under consideration in this paper is a discrete-time  $n \times n$  square MIMO system with a system model [21]

$$y = Hx + z \tag{1}$$

at the transmitter, where  $\boldsymbol{x}$  is an array of n code symbols constructed using some linear function  $\mathcal{F}(\cdot)$  on a set of information symbols v from some complex constellation  $S \subset \mathbb{Z}[\imath]$ . The elements of the channel matrix  $\boldsymbol{H}$  are i.i.d. complex Rayleigh random variables with 0 mean and unit variance and  $\boldsymbol{z}$  is the additive white Gaussian noise with 0 mean and  $\sigma^2$  variance. The received vector of code symbols is  $\boldsymbol{y}$ . For the even 2-,

4- and 8-antenna systems considered here S is assumed to be rectangular  $2^b$ -QAM with b bits per symbol. Putting the information symbols into a matrix form we have

$$\boldsymbol{V_n} = \begin{bmatrix} v_{1,1} & v_{1,2} & \dots & v_{1,n-1} & v_{1,n} \\ v_{2,1} & v_{2,2} & \dots & v_{2,n-1} & v_{2,n} \\ \vdots & \vdots & \ddots & \vdots & \vdots \\ v_{n-1,1} & v_{n-1,2} & \dots & v_{n-1,n-1} & v_{n-1,n} \\ v_{n,1} & v_{n,2} & \dots & v_{n,n-1} & v_{n,n} \end{bmatrix},$$

where n is the number of antennas in the system transmitter.

For the  $2 \times 2$  antenna case the perfect Golden Code is given in the form [2]

$$\mathbf{X_2} = \frac{1}{\sqrt{5}} \begin{bmatrix} \alpha(v_{1,1} + v_{1,2}\theta) & \alpha(v_{2,1} + v_{2,2}\theta) \\ i\overline{\alpha}(v_{2,1} + v_{2,2}\overline{\theta}) & \overline{\alpha}(v_{1,1} + v_{1,2}\overline{\theta}) \end{bmatrix}, \quad (2)$$

where  $\theta$  is the Golden number  $\frac{1+\sqrt{5}}{2}$ ,  $\overline{\theta}$  is its complement  $\frac{1-\sqrt{5}}{2}$ ,  $\alpha$  is  $1+\imath(1-\theta)$ ,  $\overline{\alpha}$  is  $1+\imath(1-\overline{\theta})$  and  $\imath$  is  $\sqrt{-1}$ . Therefore, in order to generate each layer of the STBC we must first take the rows of V and form vectors  $(v_{1,1}\ v_{1,2})^T$  and  $(v_{2,1}\ v_{2,2})^T$  which will be multiplied by the generator matrix  $R_2$  given as

$$R_2 = \begin{bmatrix} lpha & lpha heta \ \overline{lpha} & \overline{lpha} \overline{ heta} \end{bmatrix}.$$

We then arrange the product of  $\mathbf{R_2}$  and  $(v_{1,1} \ v_{1,2})^T$  along the diagonal of a  $2 \times 2$  matrix  $\mathbf{N_2}$  and the product of  $\mathbf{R_2}$  and  $(v_{2,1} \ v_{2,2})^T$  along the anti-diagonal which will give the perfect code without cubic shaping as

$$\mathbf{N_2} = \begin{bmatrix} \alpha(v_{1,1} + v_{1,2}\theta) & \alpha(v_{2,1} + v_{2,2}\theta) \\ \overline{\alpha}(v_{2,1} + v_{2,2}\overline{\theta}) & \overline{\alpha}(v_{1,1} + v_{1,2}\overline{\theta}) \end{bmatrix},$$

To achieve this shaping and create a unitary matrix we elementwise multiply the matrix  $N_2$  by  $M_2$  given as

$$M_2 = rac{1}{\sqrt{5}} \begin{bmatrix} 1 & 1 \\ i & 1 \end{bmatrix}.$$

Therefore, the final  $2 \times 2$  Golden Code carved from cubic shaped  $\mathbb{Z}[i]^2$  lattice can be written as  $X_2 = M_2 \odot N_2$  where  $\odot$  is the Hadamard product.

For the  $4 \times 4$  antenna case the perfect code in [4] is computed using the equation

$$X_4 = M_4 \odot \mathcal{L}(R_4'), \tag{3}$$

where  $R_4' = R_4 v_i^T \{1 \le i \le 4\}$  and  $v_i$  are the *i*th rows of the information symbol matrix  $V_4$ .  $R_4$  is the  $4 \times 4$  generator matrix equal to

$$\mathbf{R_4} = (\sigma_l(v_k))_{k,l=1}^4$$
.

The 4 × 4 generator matrix consists of the Galois group with generator  $\sigma_{l=1}: \omega_{15} \mapsto \omega_{15}^2$  and the basis

$$\{v_k\}_{k=1}^4 = \{(1 - 3i + i\theta, (1 - 3i)\theta + i\theta^3, -i + (-3 + 4i)\sigma + (1 - i)\sigma^3, -i + (-1 + i) - 3\theta + \theta^2 + \theta^3\}.$$

where  $\theta = \omega_{15}$  is the 15th root of unity.  $\mathcal{L}(\cdot)$  is a function that maps the products of  $\mathbf{R}_4$  and the rows of  $\mathbf{V}_4$  in a linear dispersion fashion [22] (without a loss of generality) as

$$\mathcal{L}(\mathbf{R}'_{n}) = \begin{bmatrix} r'_{1,1} & r'_{n,2} & \dots & r'_{3,n-1} & r'_{2,n} \\ r'_{2,1} & r'_{1,2} & \dots & r'_{4,n-1} & r'_{3,n} \\ \vdots & \vdots & \ddots & \vdots & \vdots \\ r'_{n-1,1} & r'_{n-2,2} & \dots & r'_{1,n-1} & r'_{n,n} \\ r'_{n,1} & r'_{n-2,2} & \dots & r'_{2,n-1} & r'_{1,n} \end{bmatrix} .$$
(4)

The 4  $\times$  4 shaping matrix  $M_4$  can be written as

$$m{M}_4 = rac{1}{\sqrt{15}} egin{bmatrix} 1 & \imath & \imath & \imath & \imath \ 1 & 1 & \imath & \imath & \imath \ 1 & 1 & 1 & \imath & \imath \ 1 & 1 & 1 & 1 \end{bmatrix}.$$

For the  $8 \times 8$  antenna case presented in [5] we can compute the generator matrix  $\mathbf{R}_8$  element-wise as

$$r_{j,k} = \omega_8^{i5^k}, \ 1 \le j, k \le 8,$$
 (5)

where j and k are the rows and column indices, respectively, of  $R_8$  and i is  $\sqrt{-1}$ . For this case  $\omega_8$  is the 8th root of unity. The code matrix  $X_8$  is computed similar to the  $4 \times 4$  case according to the equation

$$\boldsymbol{X}_8 = \boldsymbol{M}_8 \odot \mathcal{L}(\boldsymbol{R}_8'), \tag{6}$$

where  ${m R}_8' = {m R}_8 {m v}_i^T \; \{1 \leq i \leq 8\}$  and  ${m M}_8$  equals

$$m{M}_8 = rac{1}{\sqrt{8}} egin{bmatrix} 1 & \gamma \\ 1 & 1 & \gamma & \gamma & \gamma & \gamma & \gamma & \gamma \\ 1 & 1 & 1 & \gamma & \gamma & \gamma & \gamma & \gamma \\ 1 & 1 & 1 & 1 & \gamma & \gamma & \gamma & \gamma \\ 1 & 1 & 1 & 1 & 1 & \gamma & \gamma & \gamma \\ 1 & 1 & 1 & 1 & 1 & 1 & \gamma & \gamma \\ 1 & 1 & 1 & 1 & 1 & 1 & 1 & \gamma \\ 1 & 1 & 1 & 1 & 1 & 1 & 1 & 1 \end{bmatrix},$$

and  $\mathcal{L}(\cdot)$  here is the same equation as (4). It is important to note that for the  $8\times 8$  case  $\gamma$  is the non-norm element equal to 0.8-0.6i following Table I in [5].

# III. MMSE BLAST DECODING OF PERFECT SPACE-TIME CODES

At the receiver of the same  $n\times n$  square MIMO system, at each sample time, we receive the signal

$$y = Hx + z, (7)$$

which is the same form as (1). However, in order to decode any LD-based STBCs we must instead compute

$$\hat{\boldsymbol{u}} = \hat{\boldsymbol{H}}\hat{\boldsymbol{x}} + \hat{\boldsymbol{z}}.\tag{8}$$

where  $\hat{y}$  is now the  $n^2$  stacked column vector of y received symbols over n channel uses.  $\hat{H}$  denotes the  $n^2 \times n^2$  matrix

TABLE I OVER-THE-AIR TEST PARAMETERS

Parameter	Proposed System	Baseline System
Test Device	Ettus X310	Ettus X310
Daughter Cards	UBX-160	UBX-160
UHD	3.13	3.13
GNU Radio	3.7.13.4	3.7.13.4
Sample Rate	1 MHz	1 MHz
Center Freq.	2.4 GHz	2.4 GHz
FFT Size	64	64
Active Carriers	40	40
MIMO Order	$2 \times 2$	$2 \times 2$
Modulation	16-QAM	16-QAM
Channel Est.	Pilot-aided LS	Pilot-aided LS
STBC	Golden Code	None
Detector	Proposed	MMSE & BLAST
Demodulation	Hard-output	Hard-output
TX Sync	LO & CORDIC	LO & CORDIC
RX Sync	S&C algorithm	S&C algorithm

with channel matrices  $\boldsymbol{H}$  for n channel uses along its diagonal in the form

$$\hat{m{H}} = egin{bmatrix} m{H}_1 & 0 & \dots & 0 & 0 \ 0 & m{H}_2 & \dots & 0 & 0 \ dots & dots & \ddots & dots & dots \ 0 & 0 & \dots & m{H}_{n-1} & 0 \ 0 & 0 & \dots & 0 & m{H}_n \end{bmatrix}.$$

The column vector  $\hat{x}$  is a  $n^2$  stacked column vector containing n transmitted code symbol vectors x following the perfect coding principle and  $\hat{z}$  is a  $n^2$  stacked column vector of n complex Gaussian distributed noise vectors z. Since perfect codes are linear combinations of the transmitted symbols v we can re-write (8) in terms of v as

$$\hat{\mathbf{y}} = \hat{\mathbf{H}}G\hat{\mathbf{v}} + \hat{\mathbf{z}},\tag{9}$$

where G is a  $n^2 \times n^2$  generator matrix and  $\hat{v}$  is the  $n^2$  stacked column vector of n information symbol vector containing symbols from our complex constellation S.

Assuming it is possible to make an estimate of  $\boldsymbol{H}$  and the SNR at the receiver for every channel use, we can minimize the mean square error between the pre-coded information symbols  $\hat{v}_i$   $\{1 < i < n^2\}$  and the received coded symbols  $\hat{y}_i$   $\{1 < i < n^2\}$  according to the minimum mean square error (MMSE) cost function

$$\boldsymbol{M}_{\text{MMSE}} = \underset{\boldsymbol{M}}{\operatorname{argmin}} E\left(||\hat{\boldsymbol{v}} - \boldsymbol{M}\hat{\boldsymbol{y}}||^2\right). \tag{10}$$

Using the resulting rows i of  $M_{MMSE}$  as filter vectors we get

$$m_i = (BB^H + N_0 I)^{-1} b_i, \{1 < i < n^2\},$$
 (11)

where B is our "equivalent channel" over the whole space-time code given as  $B = \hat{H}G$  from (8). The *i*th column of B is  $b_i$   $\{1 < i < n^2\}$  and I is a  $n^2 \times n^2$  identity matrix.

Applying the filter to the equation (8) we can find the estimated information symbols  $\tilde{v}_i$  as

$$\tilde{v}_i = \boldsymbol{m}_i^H \hat{\boldsymbol{y}} = z_i v_i + w_i \ 1 < i < n^2,$$
 (12)

**Algorithm 1:** BLAST Optimum Ordering and SIC for Perfect Space-Time Coded MIMO.

$$\begin{array}{l} \textbf{Data: } B, \ \hat{\pmb{y}}, \ N_0 \\ \textbf{Result: } \ v' \\ o \leftarrow \text{ index of sort}(\pmb{B}), \ \text{ascending } ||\pmb{b}_j||^2; \\ i = 0; \\ \textbf{for } \ i < n^2; \ i + + \ \textbf{do} \\ & | \ o_i = o[i]; \\ \pmb{m}_{o_i} = (\pmb{B}\pmb{B}^H + N_0\pmb{I})^{-1}\pmb{b}_{o_i}; \\ \tilde{v}_{o_i} = \pmb{m}_{o_i}^H \hat{\pmb{y}}; \\ v'_{o_i} = Q(\tilde{v}_{o_i}); \\ y' = \hat{\pmb{y}} - v'_{o_i}(\pmb{B}_{o_i}); \\ \text{col}(\pmb{B}_{o_i}) = 0; \\ \hat{\pmb{y}} = \pmb{y}'; \\ \textbf{end} \end{array}$$

where  $z_i = \boldsymbol{m}_i^H \boldsymbol{b}_i$  is our complex weight scalar and  $w_i$  is the interference-plus-noise term.

In order to reduce spatial-temporal interference in our linear receiver system, we can attempt to detect each subsequent symbol estimate of  $\tilde{v}_i$  with the information from the previous detected symbols removed, therefore increasing our SNR at each detected space-time layer proportional to

$$SNR_{o_i} = \frac{E(|v_{o_i}|^2)}{\sigma^2 ||m_{o_i}||^2},$$
(13)

where the expected value is taken over the complex constellation S. Here,  $o_i$  is the optimally ordered space-time layers in our system according to the BLAST approach [23].

We first sort our equivalent space-time channel  $\boldsymbol{B}$  by the 2-norm of its columns as  $||\boldsymbol{b}_j||^2$   $\{1 < j < n^2\}$  in ascending order which gives us the optimum ordering  $o_i$ . Next we can find a symbol estimate  $v'_{o_i}$  where  $o_i$  is the i-th optimally ordered row as

$$v'_{o_i} = Q(\tilde{v}_{o_i}), \ 1 < o_i < n^2,$$
 (14)

where  $Q(\cdot)$  is a slicing function of the system constellation S. Next we can cancel this detected symbol from the original received signal vector by

$$y' = \hat{y} - v'_{o_i}(B_{o_i}), \tag{15}$$

and remove the canceled layer from the equivalent channel, creating a new "deflated" equivalent channel [23]  $\boldsymbol{B}$  by zeroing out the optimally ordered column corresponding to  $o_i$ . Lastly we set  $\hat{\boldsymbol{y}} = \boldsymbol{y}'$ . This is repeated for all  $n^2$  received symbols in optimum order iterative fashion. The overall algorithm is described in Algorithm 1.

# IV. ADAPTIVE SIC METHOD USING SYSTEM AND NOISE INFORMATION

As discussed in our previous work on adaptive detection [24], it is sometimes appropriate to target a certain error rate for some given SNR value [25] or to simply reduce complexity at the very high end of the SNR regime. Since perfect space-time coding increases the dimensionality of the (equivalent) channel at the receiver to  $n^2$ , it is important to attempt to reduce complexity

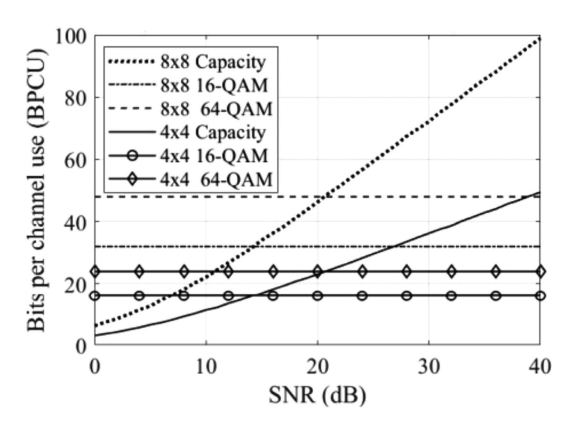


Fig. 1. MIMO system ergodic capacity of  $4\times4$  and  $8\times8$  dimensions and data rates for rectangular 16 and 64-QAM modulation.

as much as possible to maintain low latency at the receiver as matrix multiplication in general has a complexity on the order of  $O(n^3)$ . If we understand that the system data rate at some instantaneous channel use is a fraction of the theoretical capacity [1] we should be able to reduce our decoding effort correspondingly, leading to a dynamic adjustment of complexity and dynamic error performance.

Any practical MIMO system has a defined data rate in bits per channel use, R = bnr, where  $b = log_2M$  is the bits per symbol in the M-QAM complex constellation S, the number of transmit and receive antennas (spatial streams) is n, and the rate of the channel coding scheme is r. We can also compute the ergodic capacity of the space-multiplexed system [26] according to

$$C = n \log \frac{\text{SNR}_{\text{dB}}}{n}.$$
 (16)

We can plot R and C versus SNR for any practical system. Fig. 1 shows the capacity for both  $4\times 4$  and  $8\times 8$  MIMO systems along with their corresponding data rate using both 16-QAM and 64-QAM modulation. It follows that when R>C any amount of receiver processing will not reduce the error rate since we are trying to operate above capacity. On the other hand, when operating at a fraction of the ergodic channel capacity, we can apply less space-time interference cancellation proportional to this difference. Such observations have motivated us to design an adaptive interference cancellation method that is presented in the rest of this section.

In the new adaptive algorithm, we propose to dynamically adjust the number of space-time layers to cancel based on instantaneous channel conditions. More specifically, we define the dynamic number of space-time layers to cancel as

$$\lambda_{\text{dyn}} = \max\left\{ (n^2 - \lambda_{\text{red}}), 0 \right\},\tag{17}$$

where the total number of space-time layers is  $n^2$  and therefore the maximum number of successive cancellation steps.  $\lambda_{\rm red}$  is the integer value of reduction in cancellation layers according to

$$\lambda_{\text{red}} = \max\{\text{round}(\text{weight}(C - \text{offset} \cdot R)), 0\}. \tag{18}$$

The weight and offset variables are real number scalars strictly larger than 0. These values affect the speed at which the complexity is reduced and the SNR point at which the reduction

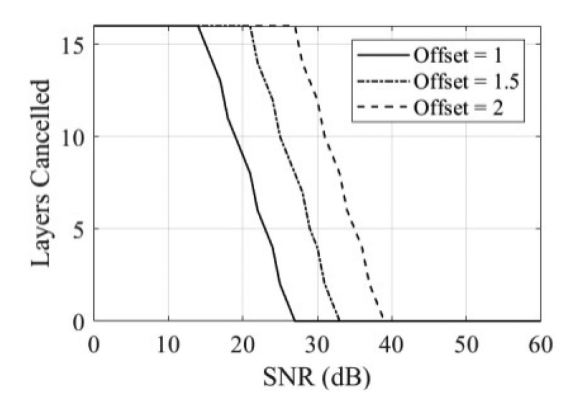


Fig. 2.  $4 \times 4$  MIMO system with 16-QAM modulation and proposed adaptive method with varying offsets and a fixed weight of 1.

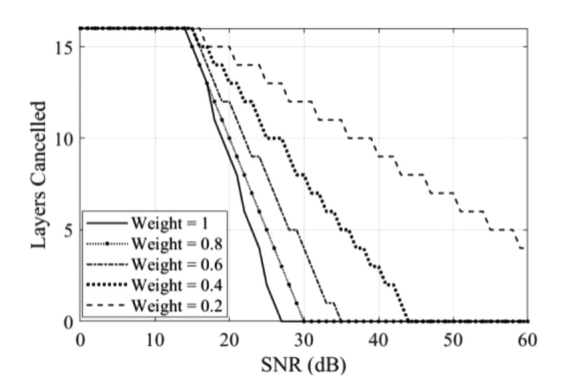


Fig. 3.  $4 \times 4$  MIMO system with 16-QAM modulation and proposed adaptive method with varying weights and a fixed offset of 1.

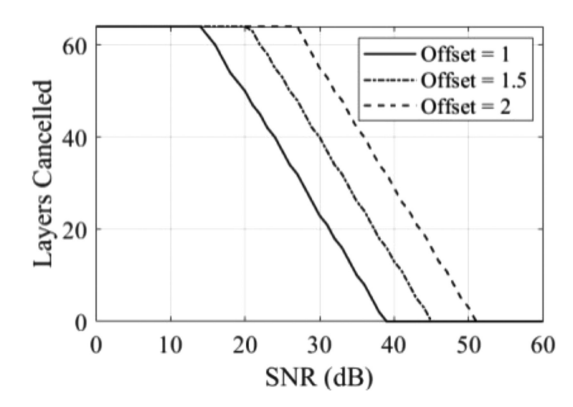


Fig. 4.  $8 \times 8$  MIMO system with 16-QAM modulation and proposed adaptive method with varying offsets and a fixed weight of 1.

starts, accordingly. Various offsets and weights are tested and their layer reduction versus SNR are plotted in Fig. 2 and Fig. 3 respectively. Fig. 4 and Fig. 5 show the same for an  $8 \times 8$  system.

The advantage of the proposed adaptive method versus simply detecting and canceling a predefined subset of space-time layers is the ability to adaptively cancel based on instantaneous channel conditions where the only fixed values are the weight and offset. The updated algorithm steps for the new adaptive method can be seen in Algorithm 2.

From the algorithm examples shown in Fig. 2–Fig. 5, we can see that the proposed adaptive method filters  $\lambda_{red}$  layers while

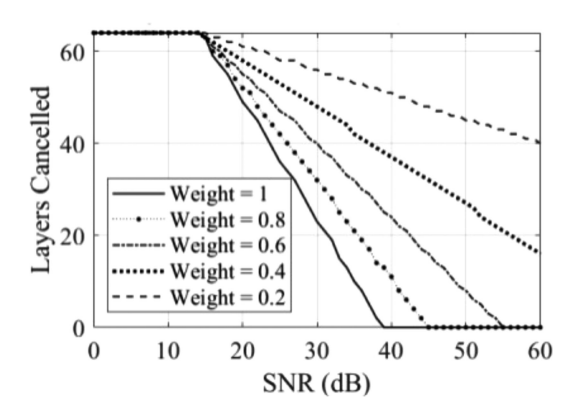


Fig. 5.  $8\times8$  MIMO system with 16-QAM modulation and proposed adaptive method with varying weights and a fixed offset of 1.

**Algorithm 2:** Adaptive BLAST Method Using Ergodic Capacity and System Rate Information.

```
Data: B, \hat{y}, N_0, C, R, weight, offset \mathbf{Result:} \ v'
o \leftarrow \mathrm{index} \ \mathrm{of:} \ \mathrm{sort}(B), ascending ||b_j||^2;
\lambda_{\mathrm{red}} = \max\{\mathrm{round}(\mathrm{weight}(C - \mathrm{offset} \cdot R)), 0\}.;
\lambda_{\mathrm{dyn}} = \max\{(n^2 - \lambda_{\mathrm{red}})\};
i = 0;

for i = 1; i < \lambda_{dyn}; i + + \mathbf{do}
\begin{array}{c} o_i = o[i]; \\ m_{o_i} = (BB^H + N_0I)^{-1}b_{o_i}; \\ \tilde{v}_{o_i} = m_{o_i}^H \hat{y}; \\ v'_{o_i} = Q(\tilde{v}_{o_i}); \\ v'_{o_i} = Q(\tilde{v}_{o_i}); \\ v' = \hat{y} - v'_{o_i}(B_{o_i}); \\ \mathrm{col}(B_{o_i}) = 0; \\ \hat{y} = y'; \\ \mathbf{end} \\ /^* \ \mathrm{one-shot} \ \mathrm{filter} \ \mathrm{remaining} \ \mathrm{layers} \ ^*/; \\ \mathbf{for} \ i = \lambda_{dyn} \ ; \ i < n^2; \ i + + \mathbf{do} \\ o_i = o[i]; \\ m_{o_i} = (BB^H + N_0I)^{-1}b_{o_i}; \\ \tilde{v}_{o_i} = m_{o_i}^H \hat{y}; \\ \mathbf{end} \end{array}
```

dynamically varying  $\lambda_{red}$  based on the provided channel and system noise information. This in-turn removes an equal number of slicer, symbol cancellation and channel zeroing steps, which affects both the error rate and runtime complexity. Although the remaining space-time layers do not need to be filtered in any particular order [23], the order is maintained since the optimum ordering indexes are already computed.

#### V. SIMULATION RESULTS AND ANALYSIS

In this research, we employed a multi-pronged approach to evaluate the performance and usefulness of the proposed adaptive BLAST method. First, extensive MATLAB simulations are used to assess the BER performance of the new adaptive method in comparison with two other well-known approaches. Second, we further implemented the detection methods in C++11 and studied run-time performance empirically to evaluate the computational complexity of the various detection methods.

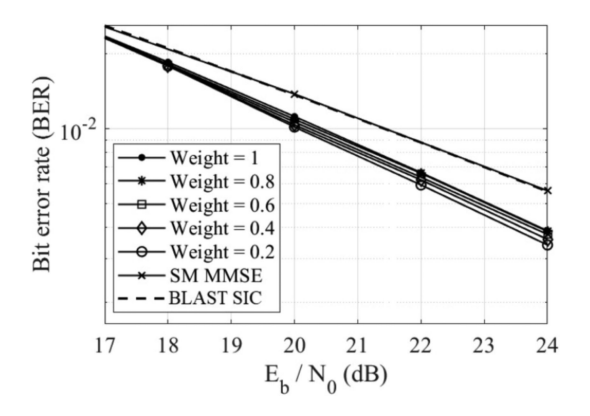


Fig. 6. BER results of a  $4 \times 4$  MIMO system with 16-QAM modulation and proposed adaptive method with varying offsets and a fixed weight of 1. SM linear detection BER is also shown for comparison.

The BER and complexity comparisons shown in this section are obtained using systems with the same throughout (BPCU). Third, we developed a custom MIMO OFDM transceiver in the GNU Radio SDR platform to evalute over-the-air performance of the proposed adaptive method.

#### A. BER Performance Results

For our BER simulations in this research, we use 10 million uncoded bits in blocks of length 1000 without channel coding in MATLAB. The input data bits are modulated using rectangular-QAM (16-QAM considered here) and then either coded using the perfect codes described in Section II or parallelized into n spatial streams.

The receiver implementations are either a one-shot linear MMSE filter, a standard MMSE BLAST optimum ordering and symbol cancellation system or our novel adaptive BLAST aproach all with perfect channel state information (CSI) as described in Section II. The estimated information symbols are demodulated using a hard-output QAM demodulator and sent directly to be checked for errors against the input bits. The SNR in dB is computed from the  $E_b/N_0$  as

$$SNR_{dB} = \left(\frac{E_b}{N_0}\right)_{dB} - 10\log_{10}\left(\frac{1}{rb}\right). \tag{19}$$

The bit energy is  $E_b$ , the noise power density is  $N_0$ , the FEC code rate is r (fixed at 1 in this research) and the bits per coded symbol is b. Lastly, we compute the linear noise variance  $\sigma^2$  as

$$\sigma^2 = 10^{\frac{-\text{SNR}_{\text{dB}}}{10}} (mE_s), \tag{20}$$

where  $E_s$  is the average symbol energy on each transmit antenna and m is the number of transmit antennas.

The simulated BER results for different offsets and weights for a  $4\times 4$  proposed system can be seen in Fig. 6 and Fig. 7, respectively. We can see that as the offset of the adaptive SIC algorithm increases the  $E_b/N_0$  point at which the diversity advantage changes is increased as well. When changing the weight of the receiver the diversity advantage changes accordingly, with low weights maintaining higher diversity throughout the  $E_b/N_0$  with a corresponding slower reduction in complexity. The same results for a  $8\times 8$  proposed system can be seen in

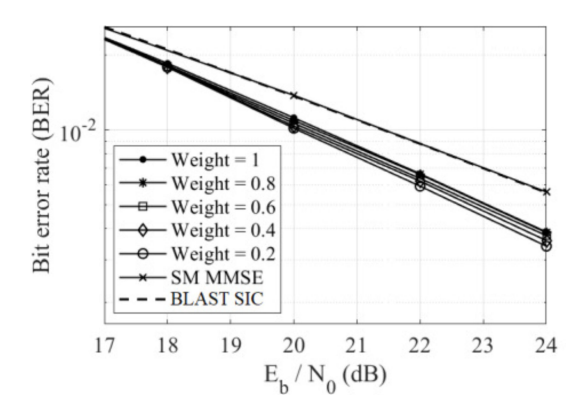


Fig. 7. BER results of a  $4 \times 4$  MIMO system with 16-QAM modulation and proposed adaptive method with varying weights and a fixed offset of 1. SM linear detection BER is also shown for comparison.

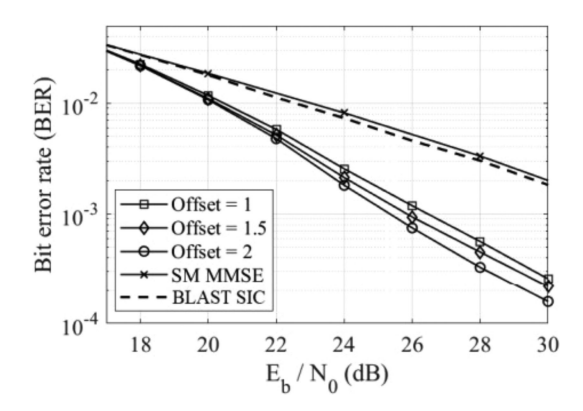


Fig. 8. BER results of a  $8 \times 8$  MIMO system with 16-QAM modulation and proposed adaptive method with varying offsets and a fixed weight of 1. SM linear detection BER is also shown for comparison.

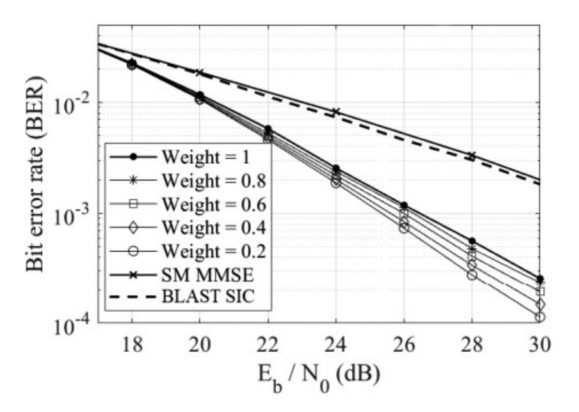


Fig. 9. BER results of a  $8 \times 8$  MIMO system with 16-QAM modulation and proposed adaptive method with varying weights and a fixed offset of 1. SM linear detection BER is also shown for comparison.

Fig. 8 and Fig. 9. Similar results to the  $4\times4$  case are observed. This makes intuitive sense since the layer cancellation is based solely on the instantaneous system information and noise meaning that the same adaptive receiver implementation can handle changing channel capacities adaptively, if needed. It follows that changing the modulation order to 4 or 64-QAM will simply update the rate information at the receiver, allowing it to adapt based on the new instantaneous difference between the channel capacity and the new rate.

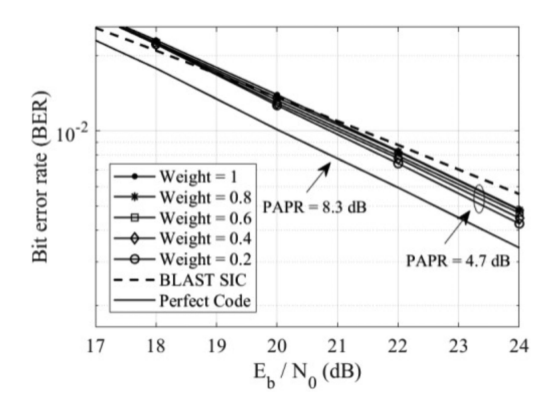


Fig. 10. BER results of a  $4 \times 4$  MIMO system with 16-QAM modulation using ICs and our adaptive method with varying weights and a fixed offset of 1. BLAST SIC BER and perfect coded BLAST SIC are also shown for comparison.

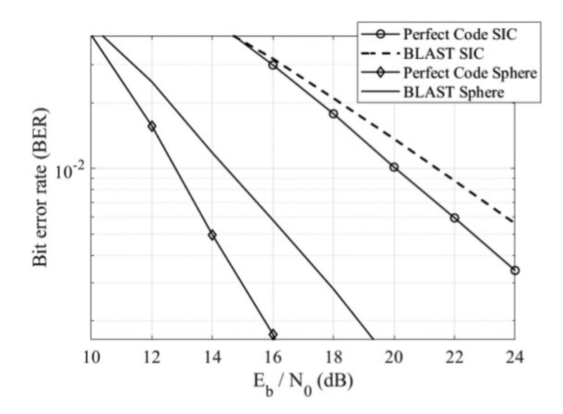


Fig. 11. BER results of a  $4\times4$  MIMO system with 16-QAM modulation using both sphere and linear MMSE SIC detection for both SM and perfect codes.

Such flexibility makes the adaptive receiver especially attractive to SDR implementations since the receiver runs on a general purpose central processing unit (CPU), which is more flexible than the more rigid field programmable gate array (FPGA) or application specific integrated circuit (ASIC) implementations. The instantaneous SNR, new rate and/or capacity can be updated very easily when the receiver function is called or when stream tags are read in SDR implementations.

To show the modularity of our proposed method, in Fig. 10, we implement ICs in a  $4 \times 4$  MIMO system using 16-QAM modulation and see that while we maintain the diversity gain of the perfect codes, we lose around 1 dB coding gain because of the minimum trace criterion used by the ICs. However, since all IC codewords are simply higher order rectangular QAM constellations, we save almost 4 dB in PAPR which is crucial to maintaining PA efficiency in mobile communication systems. Additionally, our detector is agnostic to carrier modulation meaning modified OFDM transmitters employing PAPR reduction techniques such as subcarrier shifting [27] or active constellation extension [28] can also be used. We have found in previous research that ICs with subcarrier shifting can provide a noticable improvement in OFDM PAPR [29].

Lastly, in Fig. 11 we compare ML performance of SM and perfect coding in the same  $4 \times 4$  MIMO system using 16-QAM

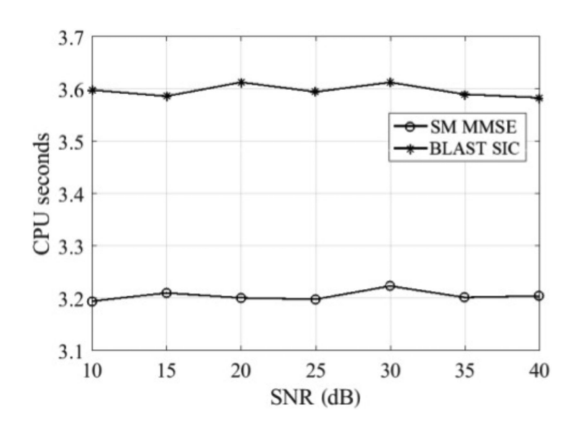


Fig. 12. CPU time versus SNR of a  $4\times4$  system using SM MMSE and BLAST SIC detectors over 1 million 16-QAM symbols.

modulation to their corresponding linear detector methods. We see that while the diversity advantage of the ML perfect coded system is around double that of the linear method, the ratio of perfect code diversity to SM diversity between the two is very close, at 1.38 and 1.77, respectively.

# B. Complexity Results

To analyze the computational complexity before further integration into the SDR framework, we have implemented the standard MMSE linear detector, the original BLAST optimum ordering and symbol cancellation method as well as our new adaptive BLAST approach in C++11 using both standard libraries and Armadillo [30], [31] linear algebra template libraries in combination with the high performance OpenBLAS (Basic Linear Algebra Subprograms) library [32]. The CPU performing the tests is an x86 based Intel Core i7-4900MQ with 8 MB of cache at an effective clock rate of 2.8 GHz. The CPU time is measured using the Armadillo timer function and the code is executed in a single thread.

We time each detector over 1 million random 16-QAM complex symbols per SNR value and average over 10 trials. The CPU timer is started after the equivalent channel B is computed. The ergodic capacity is computed offline and stored in a look-up table. It's important to remember that the perfect space-time coded system must detect  $n^2$  symbols simultaneously compared to n in the traditional SM based systems, resulting in n-times less total detection uses overall.

We first compare a SM system using BLAST optimum ordering and symbol cancellation and a standard MMSE detector. We can see in Fig. 12 that there is a noticeable increase in run-time, which is attributed to: 1) the sorting of the 2-norm of the columns of B that takes n floating point multiplications and summations and up to  $N\log_2(n)$  comparisons and replacements, 2) the slicer function that computes M floating point subtractions, where M is the complex constellation size, and 3) the symbol cancellation operation that contains both a matrix multiplication and subtraction step.

In Fig. 13, we compare the adaptive BLAST approach at low SNR versus the standard BLAST detector. We can see that there is marginal run-time increase as the overhead to compute  $\lambda_{dun}$ 

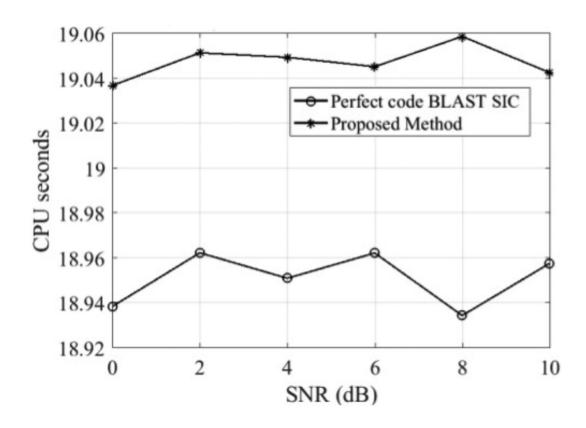


Fig. 13. CPU time versus SNR of a  $4 \times 4$  system using the purposed method and perfect coded BLAST detectors over 1 million 16-QAM symbols.

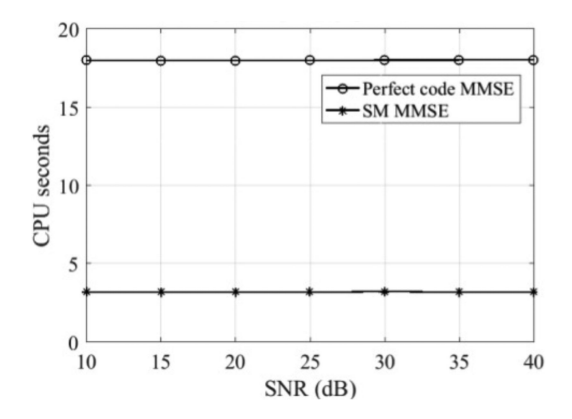


Fig. 14. CPU time versus SNR of a  $4 \times 4$  system using perfect coded MMSE and SM MMSE detectors over 1 million 16-QAM symbols.

is only 2 floating point subtractions and 2 floating point multiplications which are insignificant in comparison with matrix operations.

Next, we compare run-time increase going from SM to a perfect-coded system. In Fig. 14, we can see 1 million symbols decoded using SM MMSE and perfect-coded MMSE. Even though we call the detector n-times less, the increased matrix size significantly increases run-time. This makes intuitive sense as the computational complexity of the vector multiplication is worst-case  $\mathcal{O}(n^3)$ . Lastly, we look at the run-times of our novel adaptive BLAST approach with various weights at a fixed offset of 1 over a large range of SNR values. In Fig. 15, we can see that the run-time approaches that of MMSE (about 18 CPU seconds) as SNR increases. The complexity reduction trend follows closely Fig. 3 shown earlier in Section IV.

#### VI. IMPLEMENTATION IN THE GNU RADIO SDR FRAMEWORK

In order to properly implement our new adaptive BLAST approach over-the-air, the system needs to accurately estimate the channel matrix  $\boldsymbol{H}$  for all channel uses to further compute  $\boldsymbol{B} = \hat{\boldsymbol{H}}\boldsymbol{G}$ . In addition, the SNR and noise variance  $\sigma^2$  need to be estimated in order to adaptively cancel the space-time layers and to solve the MMSE cost function, respectively. Because of these requirements, we have developed a custom MIMO

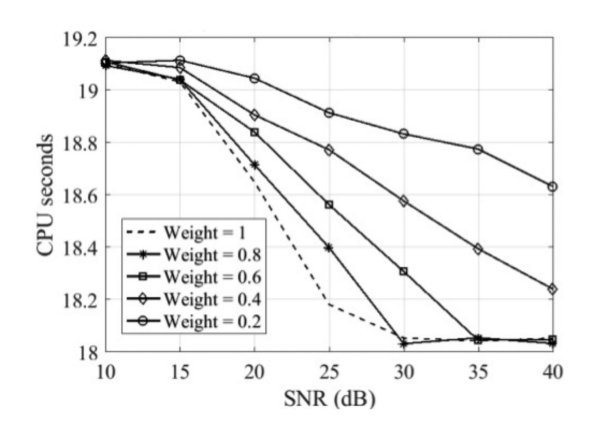


Fig. 15. CPU time versus SNR of a  $4\times4$  system using the proposed adaptive method with varying weights at a fixed offset of 1 over 1 million 16-QAM symbols.

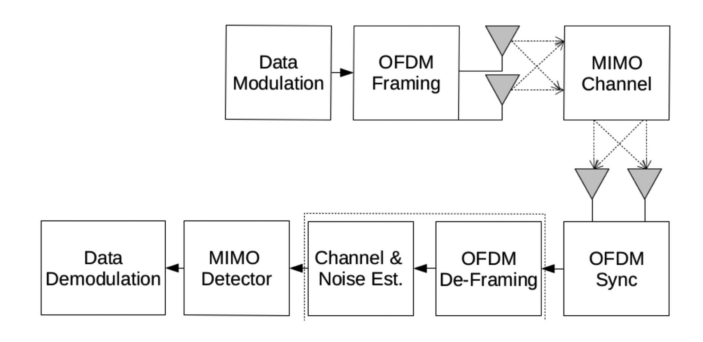


Fig. 16. Block diagram of a general MIMO OFDM system.

OFDM transceiver in the GNU Radio framework to provide these estimates to the MIMO detector. This MIMO OFDM implementation accomplishes two research goals: first, to test the performance of our proposed method using realizable suboptimum channel information as opposed to the perfect CSI assumed in Section V. Hence, the SDR system uses pilot aided, frequency domain least-squares (LS) estimation similar to LTE and WiMAX [33]. The implemention is described in detail in the following section. Second, to test performance using a more realistic channel compared to the complex Gaussian Rayleigh flat fading used throughout Section V. Although the channel is not characterized in this research, it likely follows a quasi-static Rician strong line-of-sight (LOS) frequency selective model as per the experimental setup explained in detail in this section.

#### A. Perfect Coded MIMO OFDM

For ease of explanation, the MIMO transceiver system is presented in groups of GNU Radio blocks representing basic functions of a general MIMO OFDM system like the one in Fig. 16. The data modulation is handled in Fig. 17 using either a random byte source or pre-defined byte vector feeding a chunks-to-symbol mapper which maps the bytes to 16-QAM constellation points. A transmit time tag is used to align the COordinate Rotation DIgital Computer (CORDIC) operations in the FPGA to maintain sample level coherence. The data bytes can be written to a file to be analyzed in post processing. The MIMO framing is shown in Fig. 18, where the 16-QAM

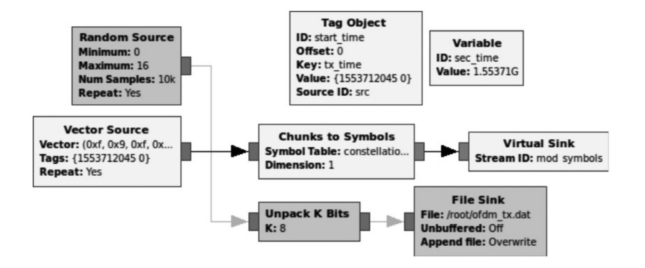


Fig. 17. Stream based 16-QAM modulation in GNU Radio with transmit time tagging for FPGA CORDIC alignment.

symbols are first perfect-coded using the  $2\times 2$  Golden Code method described in Section II and converted to 2 parallel tagged streams before adding the sync word and pilot carriers. The sync word has energy only on the odd sub carriers for use with the Schmidl and Cox (S&C) method and the pilot carriers symbols  $x_p^n$ ,  $\{1 \le p \le N_{\text{pilots}}\}$ , where  $N_{\text{pilots}} = 6$  for each stream and are drawn from non-return to zero (NRZ) Gold Code sequences. The pilots are equally spaced comb style pilots [27]. The generated OFDM frame is then converted to the time domain using the IFFT method and a cyclic prefix is prepended before being scaled by  $1/N_{\text{fft}}$  and sent to the USRP radio module. The radio interface is further phase-aligned by initializing both daughter card local oscillators (LOs) at the same time using a custom timed command approach in the GNU Radio top block.

At the receiver, the first step is OFDM synchronization which can be seen in Fig. 19. The USRP radio continuously streams samples from both daughter cards to two parallel S&C synchronizers which remove fine frequency offset and identify the beginning of the OFDM frame. The frames are tagged using this identifier signal and aligned in time. De-framing of the OFDM symbols can be seen in Fig. 20, where the cyclic prefix is removed and the OFDM frame is converted back to the frequency domain using an FFT. At the subcarrier level, if frequency offset is present, it is removed from both streams simultaneously to maintain alignment. The channel estimation is done using the LS method [21], [27] on both channels using all  $x_n^n$  pilots,  $\{1 \le p \le N_{\text{pilots}}\}$ , and further linearly interpolated to retrieve the data sub carrier gains and phases as the real and imaginary parts of  $h_{i,j,k} \in \mathbb{Z}[i]^2$ ,  $\{1 < i, j < n\}$  and  $\{1 < k < N_{\text{fft}}\}$ , respectively. The noise variance is also estimated in this block by finding the difference of 2 adjacent channel estimates and computing the variance estimate  $\hat{\hat{\sigma}}^2$  according to [34]

$$\hat{\sigma}^2 = E[((h_{i,j,k}^m - h_{i,j,k}^{m+1}) - \mu_d)^2], \quad m \ge 1, \tag{21}$$

where m is the index of the current OFDM symbol and  $\mu_d$  is the mean of the difference of the two estimates. The receiver SNR in dB can be estimated from this variance using [27]

$$S\hat{N}R_{RX} = 10 \cdot \log_{10} \left( \frac{E_{RX}}{n(N_{\text{fff}}/N_{\text{data}})\hat{\sigma}^2} \right),$$
 (22)

where  $E_{RX}$  is the energy on a single receive stream, n is the MIMO order,  $N_{\rm fft}$  is the system FFT size and  $N_{\rm data}$  is the number of data subcarriers. The variance is multiplied by  $n(N_{\rm fft}/N_{\rm data})$  since the transmitter streams are linearly combined at the receiver and not all of the OFDM subcarriers contain data, thus

maintaining the correct noise energy per transmitted information bit. The signal energy, noise variance and channel estimates are sent down stream as tags aligned to the front of each OFDM symbol. The OFDM symbols are further serialized in the sense that null carriers and pilot carriers are removed from the OFDM symbols and data carriers are converted from  $N_{\rm fft} \times 1$  vectors to parallel sample streams with a 2  $\times$  1 vector tag representing the channel states for that channel use on that specific stream.

The MIMO detection implementation can be seen in Fig. 21 which starts with channelizing the incoming  $2 \times 2$  blocks of perfect-coded symbols into  $4 \times 1$  streams and converting its respective channel states into the elements of the diagonalized equivalent channel matrix B = HG. The new channel states as  $4 \times 1$  vector tags along with signal energy and variance are sent downstream on each sample. The final step is the MIMO detection itself, which is the new adaptive BLAST method discussed in Section IV. The constructor of the GNU Radio block computes the ergodic capacity for the user defined system parameters at run time. The received SNR for each stream is computed here according to (22) and it is used to inform the BLAST detector implementing Algorithm 2 of the expected number of dynamic layer cancellation to perform according to (18). The detector is also adaptive in the sense that, if no SNR information is provided, it can perform zero-forcing (ZF) based BLAST for maximum performance given the limited information. Once the 16-QAM symbols are linearly filtered, they are passed to a hard-output demodulator that remaps the constellation points to bytes. The received data is either discarded or written to a file to be analyzed in post processing.

# B. Over-the-Air Test Results

The over-the-air test is conducted with the system parameters found in Table I on the testbed shown in Fig. 22. The SDR device is an Ettus Research X310 with two UBX-160 daughter cards running UHD 3.13. A single device ran in full duplex MIMO mode is used to emulate two half duplex MIMO devices synchronized to a common time and frequency reference like GPS. The transmit and receive antenna arrays are monopole 2.4 GHz antennas spaced 5 cm between array elements. The transmitter and receiver are spaced 25 cm apart and anchored to an acrylic optics plate for a static MIMO channel as shown in Fig. 22. The receive streams are attenuated by 30 dB using an RF attenuator to allow for testing a variety of SNR values by changing the daughter cards front end gain. The GNU Radio Companion graphical development environment allows for GUI visualization using the QT GUI interface. An example of the GUI front end developed for our system can be seen in Fig. 23 with time domain, frequency domain, received power spectrum and post-detector constellation plots.

Performance testing is conducted by starting the system and writing the transmitted and received data bits to a file for 10 seconds. Every test case is conducted at 30, 32 and 34 estimated received SNR by fixing the receiver front end gain and changing the transmitter gain in 2 dB increments. The data bits are then read into a MATLAB script where the first 10 million bits are used for a consistent BER comparison. As a baseline case, we tested a standard SM-MIMO OFDM system with both a BLAST

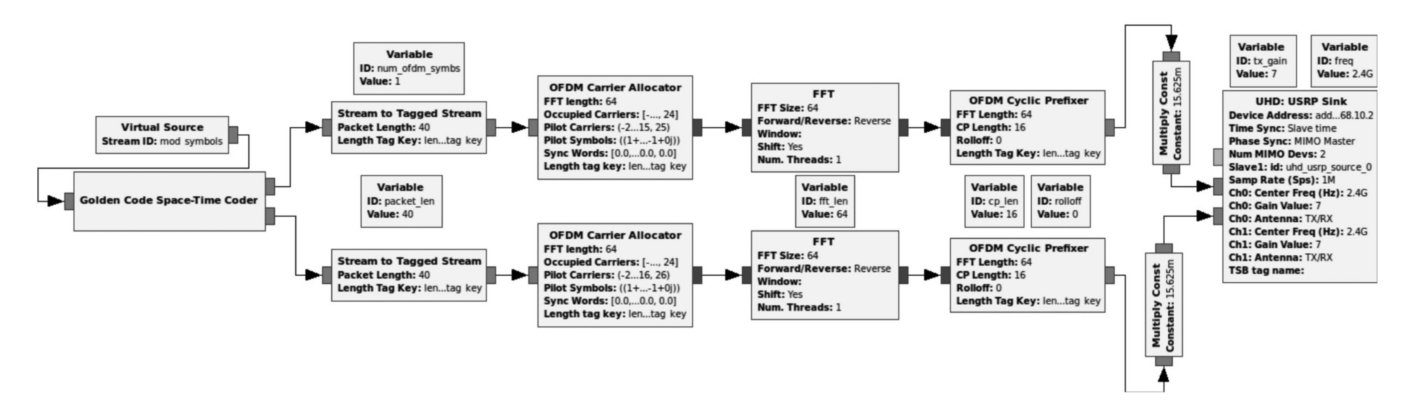


Fig. 18. Golden Code 2 × 2 MIMO OFDM transmitter in GNU Radio with automatic UBX phase alignment using a custom USRP sink.

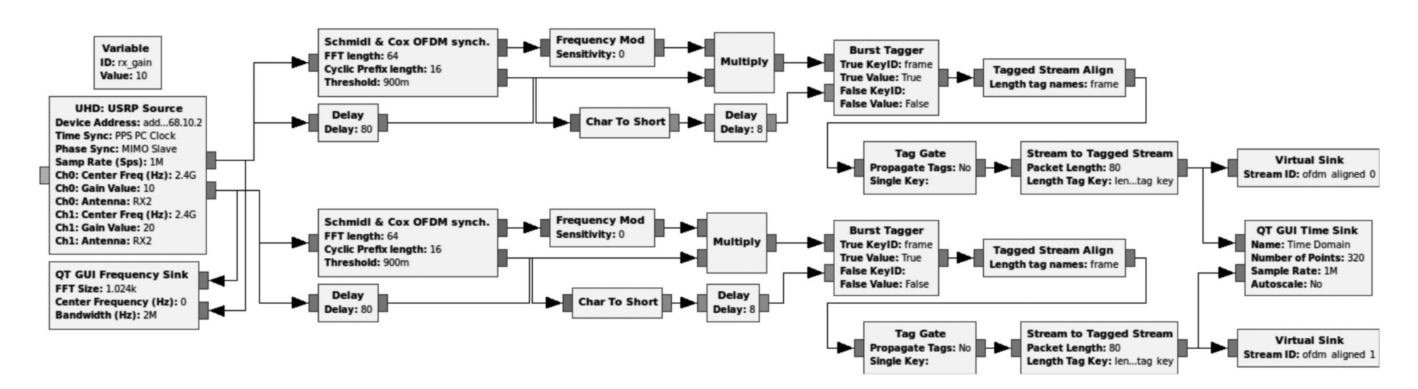


Fig. 19. Stream based 2 × 2 MIMO OFDM receive signal alignment and fine frequency correction in GNU Radio using the Schmidl and Cox synchronization method.

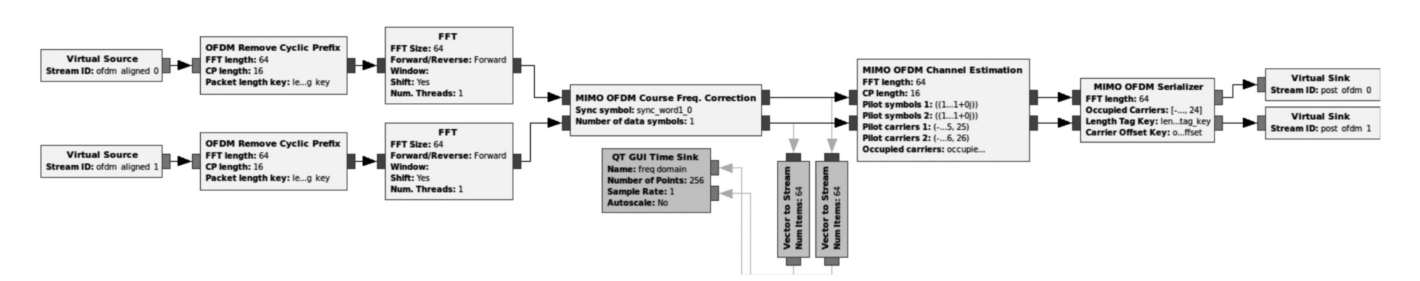


Fig. 20. 2 × 2 MIMO OFDM receiver in GNU Radio with course frequency correction and LS based pilot-aided channel and SNR estimation.

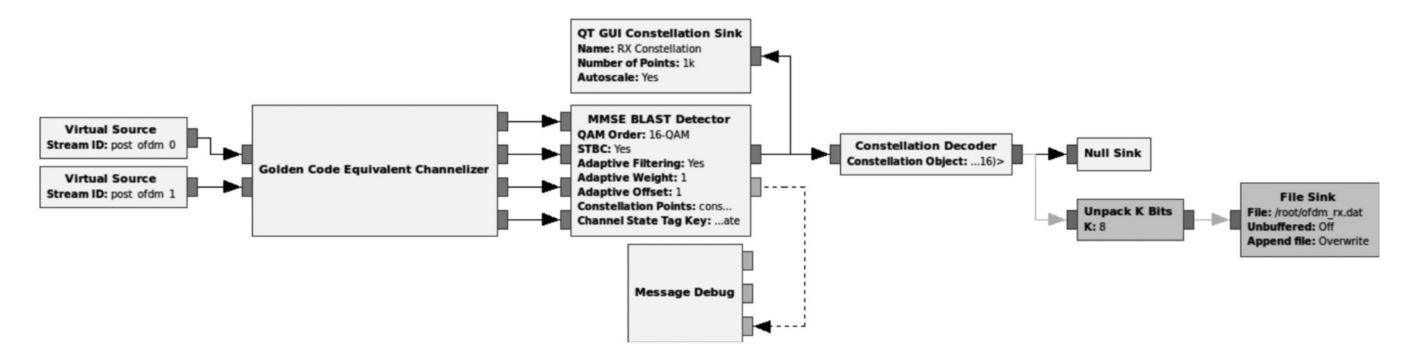


Fig. 21. Proposed adaptive BLAST based optimum ordering and SIC MIMO receiver block in GNU Radio with Golden Code 2 × 2 equivalent channelizer.

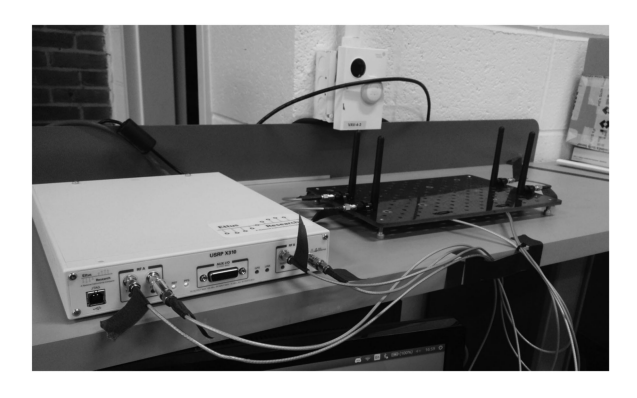


Fig. 22. Over-the-air MIMO OFDM testbed equipment: X310 with 2 UBX-160 daughter cards, 2 2.4 GHz monopole antenna arrays (transmit and receive) with elements spaced 5 cm apart. Transmitter and Receiver are spaced 25 cm apart.

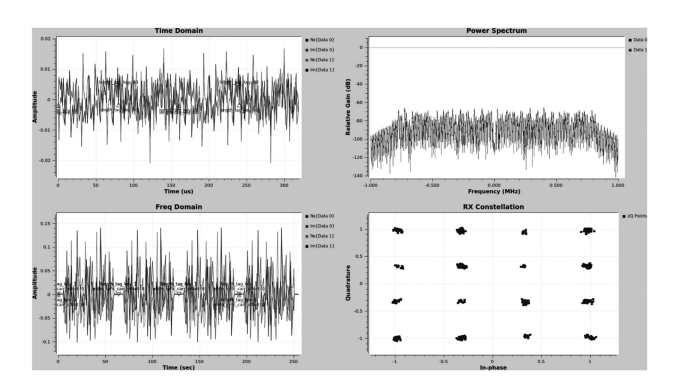


Fig. 23. GUI front end of the  $2 \times 2$  MIMO OFDM test system over-the-air at an estimated 36 dB SNR using 16-QAM modulation and Golden Code perfect space-time coding.

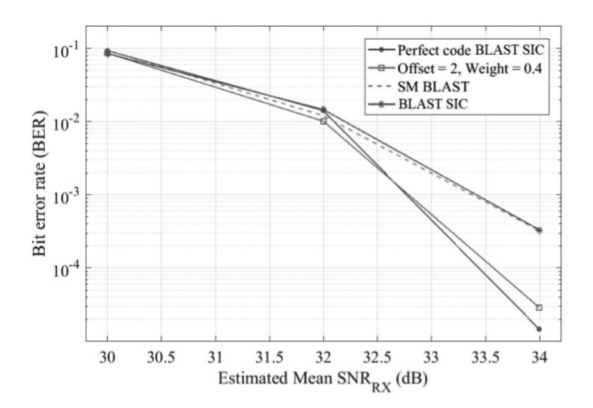


Fig. 24. BER results of the  $2\times 2$  MIMO OFDM test system over-the-air using the testbed in Fig. 22 with 16-QAM modulation, the proposed adaptive method and an SM-MIMO baseline.

and standard MMSE detector. We can see that the SM system does not gain any noticeable performance from using the BLAST method over MMSE in a  $2\times 2$  MIMO scenario. This follows our simulation results in Section V, where we only see BLAST SIC performance gains over MMSE in the  $8\times 8$  case. For the best case, we turn off the adaptive method in our detector to achieve full perfect coded BLAST performance. We can see that, even for a  $2\times 2$  system, we still achieve up to a 1 dB performance gain. To demonstrate the effectiveness of our new adaptive method, we apply an offset of 2 and a weight of 0.4 to

the adaptive layer reduction step in Algorithm 2. We see that the diversity performance decreases as the layers are dynamically canceled based on the instantaneous SNR of each OFDM data symbol. At very high SNR, the adaptive detector will perform no space-time layer cancellations ( $\lambda_{red} = n^2$ ) since the system will be operating far from capacity.

#### VII. CONCLUSION AND FUTURE RESEARCH

In this paper we have presented a novel adaptive perfect-coded MMSE BLAST based optimum ordering and SIC receiver design that allows for dynamic tuning of the diversity advantage and corresponding computational complexity using system capacity, system rate and the instantaneous SNR of the system. Through simulation results and analysis we demonstrated that the proposed system is able to handle any capacity and rate combination instantaneously at each channel use, making it attractive to SDR implementations, where this information can be passed to the receiver very easily using well established interfaces. We further analyzed the system's run-time complexity in software empirically and found that: 1) there is negligible overhead using our novel adaptive approach compared to the standard perfect-coded BLAST method, 2) larger matrix multiplications in perfect-coded receivers increase runtime by a factor of 4.5 over traditional SM systems, and 3) our proposed system can save up to 6% computational cost at high SNR. We also implemented the proposed adaptive method in the GNU Radio SDR framework using a custom developed MIMO OFDM system with the Ettus Research X310 and observed that the results are consistent with our simulation when compared to a traditional SM-MIMO OFDM system accounting for both sub-optimal LS channel estimation and a realistic frequency selective channel. This limited real world scenario testing indicates that the performance of the method will not degrade dramatically when application scenarios depart from ideal conditions slightly.

Future research efforts on this topic include: Conducting more experimental performance assessments in realistic application scenarios to fully characterize the performance of the proposed method in real system deployment. Incorporating FEC information into the detector process using an open-loop approach to maintain a highly modular design and avoid extraneous feedback from the FEC decoder, which is the standard approach [8], [35]. This FEC information will allow the detector to automaticly select the appropriate adaptive weight and offset based on a pre-defined target error rate depending on the transmitters code design and rate. Lastly, the area of machine learning, specifically reinforcement and deep learning, is gaining traction in the communications and SDR community [36] and can be leveraged to self-optimize the detector parameters after initial deployment based on learned channel conditions.

### REFERENCES

- L. Zheng and D. N. C. Tse, "Diversity and multiplexing: A fundamental tradeoff in multiple-antenna channels," *IEEE Trans. Inf. Theory*, vol. 49, no. 5, pp. 1073–1096, May 2003.
- [2] J. C. Belfiore, G. Rekaya, and E. Viterbo, "The golden code: A 2 x 2 full-rate space-time code with nonvanishing determinants," *IEEE Trans. Inf. Theory*, vol. 51, no. 4, pp. 1432–1436, Apr. 2005.

- [3] H. Yao and G. W. Wornell, "Achieving the full MIMO diversity-multiplexing frontier with rotation-based space-time codes," in *Proc. Allerton Conf. Commun.*, Control, Comput., Oct. 2003.
- [4] S. Yang, J. C. Belfiore, G. Rekaya, and B. Othman, "Perfect space-time block codes for parallel MIMO channels," in *Proc. IEEE Int. Symp. Inf. Theory*, Jul. 2006, pp. 1949–1953.
- [5] P. Elia, B. A. Sethuraman, and P. V. Kumar, "Perfect space time codes for any number of antennas," *IEEE Trans. Inf. Theory*, vol. 53, no. 11, pp. 3853–3868, Nov. 2007.
- [6] V. Tarokh, N. Seshadri, and A. Calderbank, "Space-time codes for high data rate wireless communication: Performance criterion and code construction," *Inf. Theory, IEEE Trans.*, vol. 44, no. 2, pp. 744–765, Mar. 1998.
- [7] O. Damen, A. Chkeif, and J. C. Belfiore, "Lattice code decoder for space-time codes," *IEEE Commun. Lett.*, vol. 4, no. 5, pp. 161–163, May 2000.
- [8] B. M. Hochwald and S. ten Brink, "Achieving near-capacity on a multipleantenna channel," *IEEE Trans. Commun.*, vol. 51, no. 3, pp. 389–399, Mar. 2003.
- [9] M. J. Grabner, X. Li, and S. Fu, "Performance of perfect space-time codes under linear MMSE equalization and BLAST based decoding for large data rates," in *Proc. Texas Symp. Wireless Microw. Circuits Syst.*, Apr. 2018, pp. 1–4.
- [10] G. Berhuy, N. Markin, and B. A. Sethuraman, "Fast lattice decodability of space-time block codes," in *Proc. IEEE Int. Symp. Inf. Theory*, Jun. 2014, pp. 1917–1921.
- [11] R. Vehkalahti, C. Hollanti, and F. Oggier, "Fast-decodable asymmetric space-time codes from division algebras," *IEEE Trans. Inf. Theory*, vol. 58, no. 4, pp. 2362–2385, Apr. 2012.
- [12] E. Biglieri, Y. Hong, and E. Viterbo, "On fast-decodable space-time block codes," *IEEE Trans. Inf. Theory*, vol. 55, no. 2, pp. 524–530, Feb. 2009.
- [13] A. Barreal, C. Hollanti, and N. Markin, "Fast-decodable spacetime codes for the n-relay and multiple-access MIMO channel," *IEEE Trans. Wireless Commun.*, vol. 15, no. 3, pp. 1754–1767, Mar. 2016.
- [14] B. Sethuraman, "Mutually orthogonal matrices from division algebras," J. Pure Appl. Algebra, vol. 222, no. 11, pp. 3538–3546, 2018. [Online]. Available: http://www.sciencedirect.com/science/article/pii/S0022404917303043
- [15] J. Harshan and E. Viterbo, "Integer space-time block codes for practical MIMO systems," *IEEE Wireless Commun. Lett.*, vol. 2, no. 4, pp. 455–458, Aug. 2013.
- [16] C. Xu, P. Zhang, R. Rajashekar, N. Ishikawa, S. Sugiura, Z. Wang, and L. Hanzo, "Near-perfect finite-cardinality generalized space-time shift keying," *IEEE J. Sel. Areas Commun.*, vol. 37, no. 9, pp. 2146–2164, Sep. 2019.
- [17] E. Dahlman, S. Parkvall, and J. Skold, 4G, LTE-Advanced Pro and The Road to 5G, 3rd ed. Orlando, FL, USA: Academic, 2016.
- [18] 3GPP, "NR; Physical layer; General description," 3rd Generation Partnership Project (3GPP), Sophia Antipolis Cedex, France, Tech. Specification 38.201, 2018. [Online]. Available: http://www.3gpp.org/DynaReport/ 38201.htm
- [19] E. Blossom, "GNU radio: Tools for exploring the radio frequency spectrum," *Linux J.*, vol. 2004, no. 122, p. 4, Jun. 2004. [Online]. Available: http://dl.acm.org/citation.cfm?id=993247.993251
- [20] "Ettus knowledge base: USRP hardware driver (uhd)," Ettus Res. Tech. Documentation, Nov. 2017. [Online]. Available: https://kb.ettus.com/ UHD
- [21] Proakis, Digital Communications, 5th ed. New York, NY, USA: McGraw Hill, 2007.
- [22] B. Hassibi and B. M. Hochwald, "High-rate codes that are linear in space and time," *IEEE Trans. Inf. Theory*, vol. 48, no. 7, pp. 1804–1824, Jul 2002
- [23] P. Wolniansky, G. Foschini, G. Golden, and R. Valenzuela, "V-blast: An architecture for realizing very high data rates over the rich-scattering wireless channel," in *Proc. Signals, Syst., Electron., URSI Int. Symp.*, Sep. 1998, pp. 295–300.
- [24] M. J. Grabner, X. Li, and S. Fu, "Low complexity dynamic soft-output sphere decoding based on LLR clipping and scaled Euclidean distances," in *Proc. IEEE Int. Conf. Commun.*, May 2018, pp. 1–6.
- [25] C. Studer, A. Burg, and H. Bolcskei, "Soft-output sphere decoding: Algorithms and VLSI implementation," *IEEE J. Sel. Areas Commun.*, vol. 26, no. 2, pp. 290–300, Feb. 2008.
- [26] E. Telatar, "Capacity of multi-antenna gaussian channels," Eur. Trans. Telecommun., vol. 10, no. 6, pp. 585–595, 1999.

- [27] W. Y. Y. Yong Soo Cho, J. Kim, and C. G. Kang, MIMO-OFDM Wireless Communications With MATLAB. Hoboken, NJ, USA: Wiley, 2010.
- [28] B. S. Krongold and D. L. Jones, "Par reduction in OFDM via active constellation extension," *IEEE Trans. Broadcast.*, vol. 49, no. 3, pp. 258–268, Sep. 2003.
- [29] M. J. Grabner, "Practical robust MIMO OFDM communication system for high-speed mobile communication," Master's thesis, Dept. Elect. Eng., Univ. North Texas, Denton, TX, USA, 2015.
- [30] C. Sanderson and R. Curtin, "Armadillo: A template-based C++ library for linear algebra," *J. Open Source Softw.*, vol. 1, p. 26, Jun. 2016. [Online]. Available: http://arma.sourceforge.net/armadillo\_joss\_2016.pdf
- [31] C. Sanderson and R. Curtin, "A user-friendly hybrid sparse matrix class in C++," in *Lecture Notes in Computer Science*, vol. 10931. Berlin, Germany: Springer, 2018, pp. 422–430.
- [32] W. Qian, Z. Xianyi, Z. Yunquan, and Q. Yi, "Automatically generate high performance dense linear algebra kernels on x86 cpus," in *Proc. Int. Conf. High Perform. Comput.*, Netw., Storage Anal. (SC'13), Nov. 2013.
- [33] 3GPP, "Evolved Universal Terrestrial Radio Access (E-UTRA); LTE physical layer; General description," 3rd Generation Partnership Project (3GPP), Sophia Antipolis Cedex, France, Technical Specification (TS) 36.201, 2009. [Online]. Available: http://www.3gpp.org/DynaReport/36201.htm
- [34] S. He and M. Torkelson, "Effective SNR estimation in OFDM system simulation," in *Proc. IEEE Global Commun. Conf.*, Nov. 1998, vol. 2, pp. 945–950.
- [35] K. Nikitopoulos and G. Ascheid, "Complexity adjusted soft-output sphere decoding by adaptive LLR clipping," *IEEE Commun. Lett.*, vol. 15, no. 8, pp. 810–812, Aug. 2011.
- [36] J. Ferguson, S. Kline, P. Witkowski, and S. Lisi, "Artificial intelligence radio - transceiver (air-t)," Apr. 2018. [Online]. Available: https://www. crowdsupply.com/deepwave-digital/air-t



Mitchell J. Grabner received the B.S., M.S. and Ph.D. degrees in electrical engineering from the University of North Texas, Denton, TX, USA, in 2013, 2015, and 2019 respectively. He is currently a Journeyman Research Fellow for the US Army Research Laboratory, Aberdeen Proving Ground, MD, USA. His research interests include wireless communication systems, coding and information theory, receiver design and software-defined radios.



Xinrong Li (S'00–M'04–SM'17) received the B.E. degree from the University of Science and Technology of China, Hefei, China, in 1995, the M.E. degree from the National University of Singapore, Singapore, in 1999, and the Ph.D. degree from Worcester Polytechnic Institute (WPI), Worcester, MA, USA, in 2003, all in electrical engineering. From 2003 to 2004, he was a Postdoctoral Research Fellow with the Center for Wireless Information Network Studies, WPI. He has been working with the Department of Electrical Engineering, University of North Texas,

Denton, Texas, as an Assistant Professor since 2004, and an Associate Professor since 2010. His research has been focused on statistical signal processing, real-time embedded system, and wireless sensor network.



Shengli Fu received the B.S. and M.S. degrees in telecommunication engineering from the Beijing University of Posts and Telecommunications, Beijing, China, in 1994 and 1997, respectively, the M.S. degree in computer engineering from Wright State University, Dayton, OH, USA, in 2002, and the Ph.D. degree in electrical engineering from the University of Delaware, Newark, DE, USA in 2005. He is currently a Professor and the Chair with the Department of Electrical Engineering, University of North Texas, Denton, TX, USA. His research interests include

coding and information theory, wireless communications and sensor networks, aerial communication, and UAS networks.